Andreas Jäger[a], Roman Lackner[a,b]

[a] Institute for Mechanics of Materials and Structures, Vienna University of Technology, Vienna, Austria
[b] Computational Mechanics, Technical University of Munich, Munich, Germany

Identification of viscoelastic model parameters by means of cyclic nanoindentation testing

A method for the identification of model parameters describing the time-dependent material behavior by means of cyclic nanoindentation is presented. The complex shear modulus of the material sample is determined from the prescribed amplitude in the load history, the measured amplitude in the penetration history, and the phase shift between the peak values for the load and the penetration. The parameters for a specific viscoelastic model are obtained by comparing the experimentally-obtained storage and loss moduli – both depending on the frequency used during cyclic testing – with the analytical expressions for the respective viscoelastic model. The presented method is applied to low-density polyethylene, giving access to the parameters of the fractional dash-pot which is used to describe the viscoelastic behavior. The results are compared with results from nanoindentation (static) creep tests, considering different maximum loads. Finally, the performance of the presented method is assessed by comparing the creep-compliance functions corresponding to the model parameters identified by nanoindentation with the macroscopic creep-compliance function obtained from bending-beam-rheometer tests.

Keywords: Viscoelasticity; Creep; Cyclic nanoindentation; Parameter identification; Polymers

1. Introduction

The nanoindentation technique is a well known tool for the identification of mechanical properties at the micro- and nanometer scale of materials. In the case of elastic or elastoplastic materials, Young's modulus can be determined from the unloading phase of the nanoindentation test [1]. Recently, methods for the identification of viscoelastic properties from materials exhibiting time-dependent response have been developed (see, e. g., [2–8]). In these the measured increase of the penetration during the so-called holding phase is compared with the respective analytical solution for the mathematical problem of a rigid indenter penetrating a viscoelastic halfspace [9]. Another method for the identification of viscoelastic parameters is characterized by cyclic loading [1, 10–13]. Here an oscillating load is applied to the tip and the amplitude of the penetration history and phase shift between the peak values for the penetration and the prescribed load history is measured. With these two parameters, the complex modulus and the phase angle of the material sample can be determined. Cyclic nanoindentation has been applied in several studies for the mechanical characterization of polymers [14–18]. In all these publications, the viscoelastic behavior of the polymers was, if at all, described by a Kelvin–Voigt model.

In this paper, a tool for identification of parameters for various linear viscoelastic models, representing the time-dependent behavior of the material sample, is presented. For this purpose, the modeling of the dynamic response of the nanoindentation system in terms of complex stiffnesses is dealt with in the following section. Moreover, based on the complex stiffness of the whole system, determined from the measured load and penetration amplitude and the phase shift, the complex shear moduli of the tested material sample will be extracted, giving access to the parameters for a chosen viscoelastic model. The presented technique for parameter identification is illustrated for low-density polyethylene, with the material and testing specifications given in Section 3. In order to assess the performance of the method, the obtained model parameters are compared with results from nanoindentation (static) creep tests and bending-beam-rheometer tests given in Section 4.

2. Cyclic nanoindentation testing

During cyclic nanoindentation testing, the indenter tip is loaded by a constant load $\bar{P}$ superimposed by a sinusoidal cyclic load, giving a total load of $P(t) = \bar{P} + P_0 \sin(\omega t)$, with P_0 as the load amplitude and $\omega = 2\pi f$ as the angular frequency (f is the cyclic frequency). The amplitude of the penetration history and the phase shift between the peak values of the load and the penetration history are recorded. Both test results depend not only on the tip-sample interaction but also on the dynamic behavior of the experimental set-up (see Fig. 1). Whereas the load frame can be modeled as a spring with the stiffness c_f (N m^{-1}), the mechanical behavior of the transducer controlling the applied load is approximated by a Kelvin–Voigt element, with the spring stiffness c_t (N m^{-1}) and the damping coefficient D_t (N s m^{-1}). The mass of the indenter tip m (g) and the parameters c_f, c_t, and D_t are determined during the calibration of the nanoindentation-testing equipment [19]. Finally, the interaction between the indenter tip and the sample material within the mechanical model depicted in Fig. 1b is considered by the contact stiffness S (N m^{-1}), given by

$$S\frac{\mathrm{d}P}{\mathrm{d}h} = 2M\frac{\sqrt{A_c}}{\sqrt{\pi}} \tag{1}$$

where P(N) is the load, h(m) is the penetration, M (GPa) is the indentation modulus, and A_c(m^2) is the contact area. The penetration history, $h(t)$, resulting from the sinusoidal

MK_mk-101706 – 18.6.08/druckhaus köthen

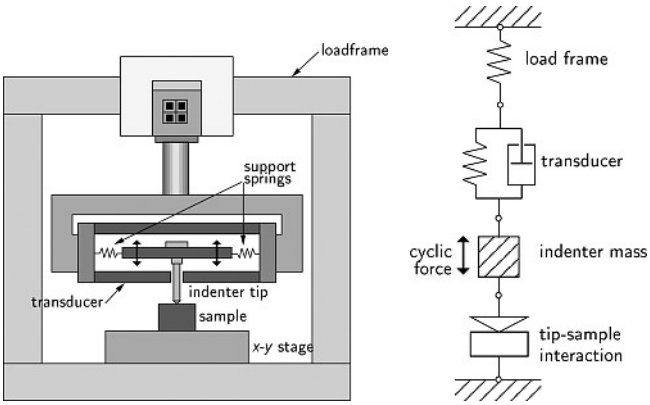

(a) (b)

Fig. 1. (a) Nanoindentation system and (b) mechanical representation of different components.

loading is given by

$$h(t) = h_0 \sin(\omega t - \varphi) \tag{2}$$

where h_0 is the amplitude of the penetration history and φ is the phase angle. The ratio between the amplitude in the prescribed force history and the measured penetration history gives the complex stiffness of the mechanical model as

$$\frac{F_0}{h_0(\omega)} = |c^*_{\text{total}}(\omega)| = |c'_{\text{total}}(\omega) + ic''_{\text{total}}(\omega)| = \sqrt{c'^2_{\text{total}}(\omega) + c''^2_{\text{total}}(\omega)} \tag{3}$$

with c'_{total} and c''_{total} as the total storage and loss stiffness, respectively. The phase angle φ is defined by

$$\tan\varphi(\omega) = \frac{c''_{\text{total}}(\omega)}{c'_{\text{total}}(\omega)} \tag{4}$$

Based on the mechanical model given in Fig. 2, the complex stiffness is given by

$$c^*_{\text{total}}(\omega) = S^*(\omega) + cm^*(\omega) + c^*_{\text{f+t}}(\omega) \tag{5}$$

where S^* (N m^{-1}) and $c^*_{\text{f+t}}$ (N m^{-1}) represent the complex stiffness of the tip–sample interaction and the nanoindentation-testing equipment, respectively, and

$$c^*_{\text{m}}(\omega) = -m\omega^2 \tag{6}$$

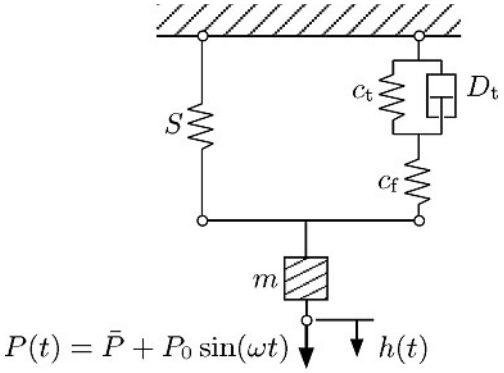

Fig. 2. Mechanical model representing the nanoindentation system loaded by cyclic force $P(t)$.

accounts for the inertia of the indenter mass, with $c'_{\text{m}} = -m\omega^2$ and $c''_{\text{m}} = 0$. The storage and loss stiffness corresponding to the complex stiffness of the nanoindentation-testing equipment, $c^*_{\text{f+t}}$, are obtained as (see, e. g., [20])

$$c'_{\text{f+t}}(\omega) = \frac{c_{\text{f}}c_{\text{t}}(c_{\text{f}} + c_{\text{t}}) + D_{\text{t}}^2 c_{\text{f}}\omega^2}{(c_{\text{f}} + c_{\text{t}})^2 + D_{\text{t}}^2\omega^2} \quad \text{and}$$

$$c''_{\text{f+t}}(\omega) = \frac{(c_{\text{f}} + 2c_{\text{t}})c_{\text{f}}D_{\text{t}}\omega}{(c_{\text{f}} + c_{\text{t}})^2 + D_{\text{t}}^2\omega^2} \tag{7}$$

Assuming the stiffness of the load frame to be much higher than the stiffness of the transducer, setting $c_{\text{f}} = \infty$, the storage and loss stiffness given in Eqs. (7) reduce to

$$c'_{\text{f+t}} = c_{\text{t}} \quad \text{and} \quad c''_{\text{f+t}}(\omega) = D_{\text{t}}\omega \tag{8}$$

In the case of elastic material response and assuming a rigid indenter tip, the indentation modulus M appearing in Eq. (1) for the contact stiffness S can be expressed by the bulk modulus K and the shear modulus μ_0, reading

$$M = \frac{E}{1 - \nu^2} = 4\mu_0 \frac{3K + \mu_0}{3K + 4\mu_0} \tag{9}$$

For $K = \infty$, $M = 4\mu_0$ representing the special case of incompressible material behavior. The complex contact stiffness representing the tip–sample interaction is obtained by replacing the indentation modulus M in Eq. (1) by the complex indentation modulus M^* of the viscoelastic model representing the material sample, reading for the case of incompressible materials

$$S^* = 2M^* \frac{\sqrt{A_{\text{c}}}}{\sqrt{\pi}} = 8\mu^* \frac{\sqrt{A_{\text{c}}}}{\sqrt{\pi}} \tag{10}$$

with the storage and loss stiffness given as

$$S' = 8\mu' \frac{\sqrt{A_{\text{c}}}}{\sqrt{\pi}} \quad \text{and} \quad S'' = 8\mu'' \frac{\sqrt{A_{\text{c}}}}{\sqrt{\pi}} \tag{11}$$

Finally, the storage and loss stiffness of the whole mechanical model are given by

$$c'_{\text{total}}(\omega) = 8\sqrt{\frac{A_{\text{c}}}{\pi}}\,\mu'(\omega) - m\omega^2 + c_{\text{t}} \quad \text{and}$$

$$c''_{\text{total}}(\omega) = 8\sqrt{\frac{A_{\text{c}}}{\pi}}\mu''(\omega) + D_{\text{t}}\omega \tag{12}$$

In order to identify the underlying rheological model describing the time-dependent behavior of the material sample and, finally, to identify the respective model parameters, the complex moduli for different viscoelastic models are determined from the Laplace–Carson transformation of the creep-compliance function $J(t)$ and provided in Tables 1 and 2.

The still unknown model parameters describing the viscoelastic behavior of the material sample are determined from the experimentally obtained complex stiffness c^*_{total} and the phase angle φ, both being a function of the pre-spe-

Table 1. Creep-compliance function for different viscoelastic models.

Model	Creep-compliance function $J(t)$
Spring	$1/\mu_0$
Dash-pot	t/η
Maxwell	$1/\mu_0 + t/\eta$
Kelvin–Voigt	$1/\mu_0(1-\exp(-\mu_0 t/\eta))$
Burgers	$1/\mu_0 + 1/\mu_v(1-\exp(-\mu_v t/\eta_v)) + t/\eta$
Fractional dash-pot	$J_a(t/\tau)^k$
Power law	$J_0 + J_a(t/\tau)^k$

Table 2. Storage and loss moduli for viscoelastic models listed in Table 1.

Model	Storage modulus μ'	Loss modulus μ''
Spring	μ_0	0
Dash-pot	0	$\eta\omega$
Maxwell	$\dfrac{\eta^2\omega^2/\mu_0}{1+\eta^2\omega^2/\mu_0^2}$	$\dfrac{\eta\omega}{1+\eta^2\omega^2/\mu_0^2}$
Kelvin–Voigt	μ_0	$\eta\omega$
Burgers*	$\dfrac{p_1q_1\omega^2 - q_2\omega^2(1-p_2\omega^2)}{p_1^2\omega^2+(1-p_2\omega^2)^2}$	$\dfrac{p_1q_2\omega^3 + q_1\omega(1-p_2\omega^2)}{p_1^2\omega^2+(1-p_2\omega^2)^2}$
Fractional dash-pot	$\dfrac{1}{J_a}\dfrac{\omega^k}{\Gamma(1+k)}\cos\left(\dfrac{k\pi}{2}\right)$	$\dfrac{1}{J_a}\dfrac{\omega^k}{\Gamma(1+k)}\sin\left(\dfrac{k\pi}{2}\right)$
Power law	$\dfrac{J_0 + J_a\Gamma(1+k)\omega^{-k}\cos\left(\dfrac{k\pi}{2}\right)}{J_0^2 + 2J_0J_a\Gamma(1+k)\omega^{-k}\cos\left(\dfrac{k\pi}{2}\right) + J_a^2\Gamma^2(1+k)\omega^{-2m}}$	$\dfrac{J_a\Gamma(1+k)\omega^{-k}\sin\left(\dfrac{k\pi}{2}\right)}{J_0^2 + 2J_0J_a\Gamma(1+k)\omega^{-k}\cos\left(\dfrac{k\pi}{2}\right) + J_a^2\Gamma^2(1+k)\omega^{-2k}}$

* $p_1 = \eta/\mu_0 + \eta/\mu_v + \eta_v/\mu_v$, $p_2 = (\eta\eta_v)/(\mu_0\mu_v)$, $q_1 = \eta$, $q_2 = (\eta\eta_v)/\mu_v$

cified angular frequencies ω, according to the procedure outlined in Fig. 3.

Remark 1: The change in the contact area A_c with time was not considered. Since the penetration amplitude corresponding to the oscillating part of the load history, $P_0\sin(\omega t)$, is in the range of only a few nanometers (commonly 1–3 nm), the variation of the contact area is negligible.

Remark 2: The creep deformation associated with the constant part of the load history, $\bar{P}$, on the other hand, results in a continuous increase in the contact area. During the nanoindentation test, the contact area is computed as a mean value over several load cycles. If the material shows asymptotic creep (as in case of the polymer considered in this paper) and the number of load cycles considered for determination of c^*_{total} and φ is small, the influence of the creep deformation associated with $\bar{P}$ can be neglected. However, one should keep in mind that, especially for small penetrations, the change in the contact area may influence the identified model parameters.

3. Materials and experimental program

In this study, low-density polyethylene (LDPE), with its Young's modulus ranging from 0.139 to 0.35 GPa (see, e. g., [21]), and a Poisson's ration of 0.39 is considered. Nanoindentation tests were conducted at room temperature using a Hysitron Triboindenter nanoindenter with a three-sided Berkovich diamond tip and a cono-spherical tip with a nominal tip radius of 5 µm. The area functions for both tip shapes were obtained by the standard calibration procedure outlined in [1] using fused quartz (FQ) as the calibration material. All tests were performed in the nanoDMA© module, where the tip is loaded by a constant load $\bar{P}$ and a cyclic load at a predefined frequency, with $P = \bar{P} + P_0\sin(\omega t)$. Tests were conducted for frequencies ranging from 15 to 170 Hz. For each frequency, c^*_{total} and φ are computed from 100 load cycles. In addition to the frequency and the amplitude P_0, $\bar{P}$ was varied in the experimental program (see Table 3). For each $(\bar{P}, P_0)$-pair, nine indents were performed.

4. Results and discussion

Figures 4 and 5 show the mean values of the storage and loss shear moduli, μ'_{exp} and μ''_{exp}, obtained from cyclic nanoindentation testing for different frequencies and different values of $\bar{P}$. For the Berkovich tip, both the mean values and the standard deviation of the storage and loss modulus decrease with increasing load. The same trend of the material parameters for an increased load $\bar{P}$ and, consequently, an increased penetration were observed during nanoindentation (static) creep tests. This behavior may be explained by the microstructure of LDPE, characterized by crystals

1. Determine c'_{total} and c''_{total} using Eqs. (3) and (4) for the considered frequencies ω_i, reading

$$c'_{\text{total}}(\omega_i) = |c^*_{\text{total}}(\omega_i)| \cos\varphi(\omega) \quad \text{and}$$

$$c''_{\text{total}}(\omega_i); = |c^*_{\text{total}}(\omega_i)| \sin\varphi(\omega) \tag{13}$$

2. Compute storage and loss shear moduli of the material sample from Eqs. (12) as

$$\mu'_{\text{exp}}(\omega_i) = \frac{1}{8}\sqrt{\frac{\pi}{A_c}}[c'_{\text{total}}(\omega_i) + m\omega_i^2 - c_t] \quad \text{and}$$

$$\mu''_{\text{exp}}(\omega_i) = \frac{1}{8}\sqrt{\frac{\pi}{A_c}}[c''_{\text{total}}(\omega_i) - D_t\omega_i] \tag{14}$$

Hereby, the parameters m, c_t, and D_t are obtained from the calibration of the system. The contact area A_c is computed from the contact height h_c, with $h_c = h - 0.75\bar{P}/S'$.

3. Identify the parameters for the chosen viscoelastic model by minimizing the error between the experimentally-obtained shear moduli (Eqs. (14)) and the expressions for the viscoelastic models given in Table 2, with the model parameters as unknowns. For the case of the fractional dash-pot model, the error

$$R = \frac{e(J_a, k)}{u} \tag{15}$$

with

$$e^2(J_a, k) = \sum_{i=1}^{n}[(\mu'_{\text{exp}}(\omega_i) - \mu'_{\text{model}}(J_a, k, \omega_i))^2 + (\mu''_{\text{exp}}(\omega_i) - \mu''_{\text{model}}(J_a, k, \omega_i))^2] \tag{16}$$

and

$$u^2 = \sum_{i=1}^{n}[\mu'_{\text{exp}}(\omega_i)^2 + (\mu''_{\text{exp}}(\omega_i)^2] \tag{17}$$

is minimized during identification of model parameters, where n is the number of different frequencies considered in the nanoindentation-testing program. In Eqs. (15) and (16), J_a is the initial creep compliance and k is the creep exponent of the fractional dash-pot model, with $0 \leq k \leq 1$.

Fig. 3. Flowchart for identification of model parameters from cyclic nanoindentation tests.

Table 3. Constant and oscillating part of load histories considered in the experimental program.

Tip	$\bar{P}/P_0$ (μN)					
Berkovich	5/0.2	10/0.2	20/0.2	50/1.0	100/2	200/5
Cono-spherical	5/0.2	10/0.2	20/0.2	–	–	–

with a lamellar thickness of the order of 10 nm embedded in an amorphous phase [22]. Thus, with increasing penetration, the effective material behavior is measured and the influence of the LDPE microstructure decreases. The results obtained from cyclic testing with the cono-spherical tip show the same dependence of the material parameters on the penetration.

The viscoelastic behavior of LDPE is described by a fractional dash-pot, which was employed in [23] for parameter identification from nanoindentation (static) creep tests. For each set of nine indents, the parameters for the fractional dash-pot, the initial creep compliance J_a and the creep exponent k, were determined and mean values for both parameters were computed. Figure 6 shows a comparison between the experimental results and the respective model response for the storage and loss modulus, μ' and μ'', as a function of the cyclic frequency f. The good agreement between the experimental results and the model response for the storage and loss modulus confirms the proper choice of the fractional dash-pot for representing the viscoelastic response of LDPE.

In order to assess the results obtained from cyclic testing, the identified model parameters are compared with data from static creep tests. As regards the latter, parameter identification from nanoindentation (static) creep tests is based on the measured increase of penetration during the so-called holding phase of the measured penetration history [8, 24] (see Fig. 7a). In case of materials showing – in addition to viscoelastic – also plastic material response, the plastic deformation might be considered by the application of the so-called double-indentation technique [23]. Here, the effect of plastic deformation is determined by adapting the experimental set-up (change of load history, see Fig. 7b) and considered in the employed parameter identification scheme. For a detailed description of both methods, the reader is referred to [8, 23].

Figure 8 shows the mean values of the identified model parameters for LDPE as a function of the maximum penetration, for both static creep tests (single- and double-indentation technique, see [23]) and cyclic testing using both tip

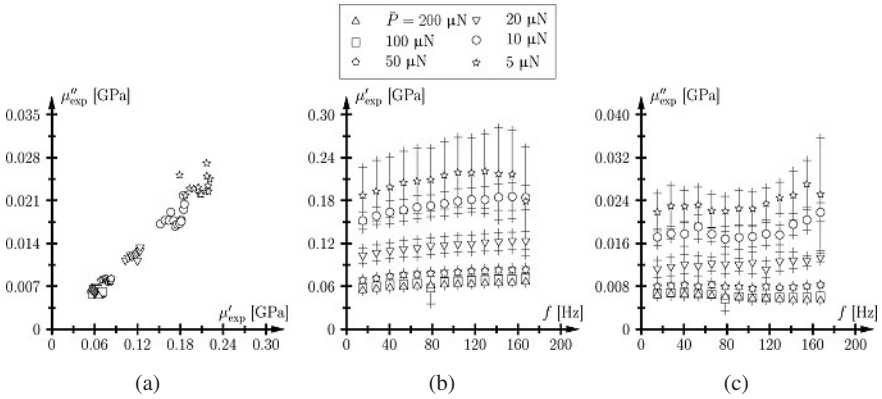

Fig. 4. (a) Cole–Cole diagram, mean values and standard deviation for (b) storage modulus μ'_{exp} and (c) loss modulus μ''_{exp} as a function of frequency for different values of $\bar{P}$ (Berkovich tip).

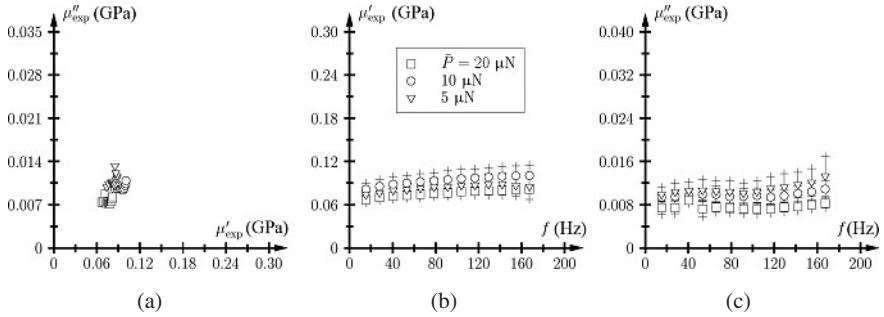

Fig. 5. (a) Cole–Cole diagram, mean values and standard deviation for (b) storage modulus μ'_{exp} and (c) loss modulus μ''_{exp} as a function of frequency for different values of $\bar{P}$ (cono-spherical tip).

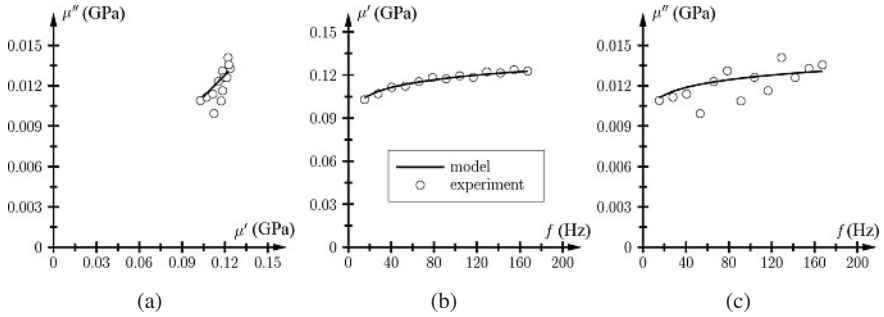

Fig. 6. Comparison of experimental results and model response obtained from parameter idfentification: (a) Cole–Cole diagram, (b) storage modulus μ', and (c) loss modulus μ'' (experimental data for $\bar{P} = 20$ μN and $P_0 = 0.2$ μN).

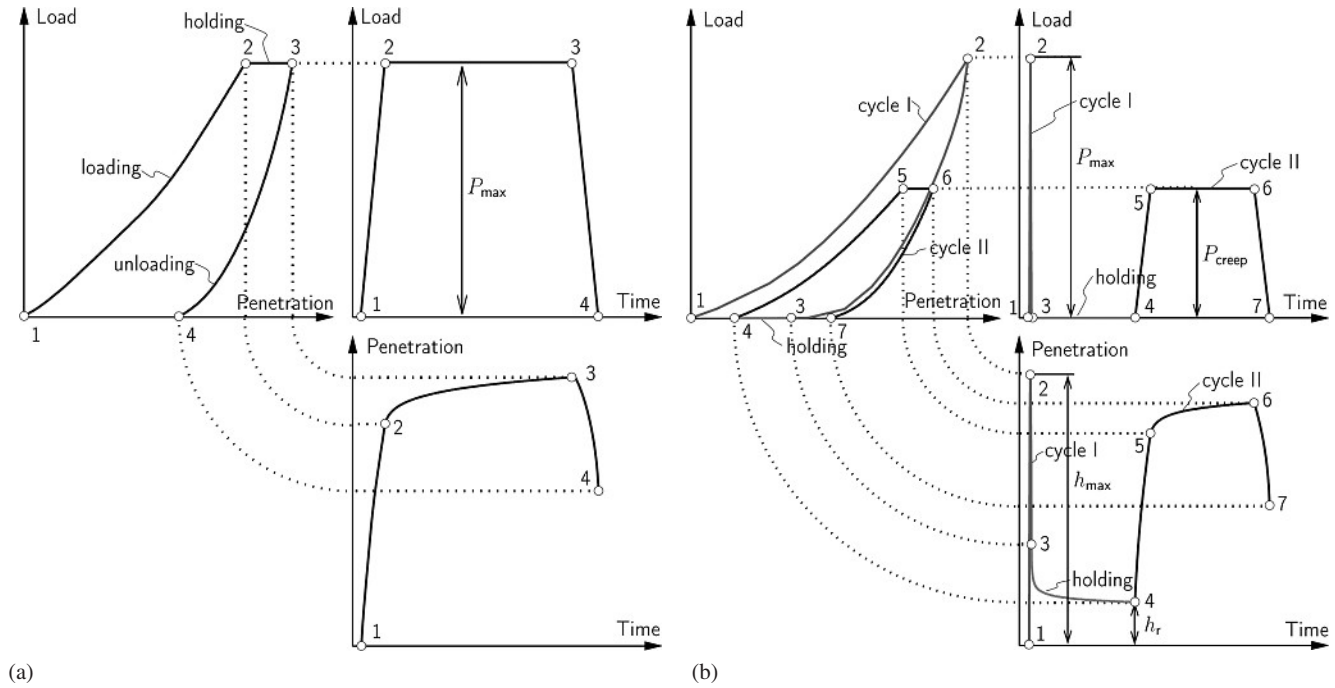

Fig. 7. Load–penetration curve, load history, and penetration history for (a) single-indentation test and (b) double-indentation test on material exhibiting elastic, viscous, and plastic material response [23].

shapes. As regards the results obtained by the Berkovich tip, both the single- and double-indentation technique reveal a similar load dependence of J_a and k, reaching a constant value of both parameters as the maximum load increases. This load dependence highlights again the influence of the LDPE microstructure on the measured material behavior. Comparing the obtained parameters, the single-indentation technique is found to overestimate the initial creep compliance, which is explained by the occurrence of plastic deformation assigned to the viscoelastic behavior during parameter identification. The creep exponent, on the other hand, is approximately the same for both techniques.

The creep tests conducted with the cono-spherical tip only give reliable results for small penetration depths [23]. The approximation of the tip shape in the employed parameter-identification scheme is not able to describe the complex tip shape for higher penetration depth. Hence, only tests conducted with small loads, characterized by a maximum penetration of about 150 nm, give reliable results.

The mean values of the fractional dash-pot parameters determined by cyclic testing are in good agreement with the parameters determined from the nanoindentation (static) creep tests. As regards the Berkovich tip, the same increase in the initial creep compliance J_a with increasing penetration was found. Also, the values for the creep exponent k correspond well for all three methods.

In order to assess the identified model parameters, the creep-compliance function $J(t)$ for the fractional dash-pot

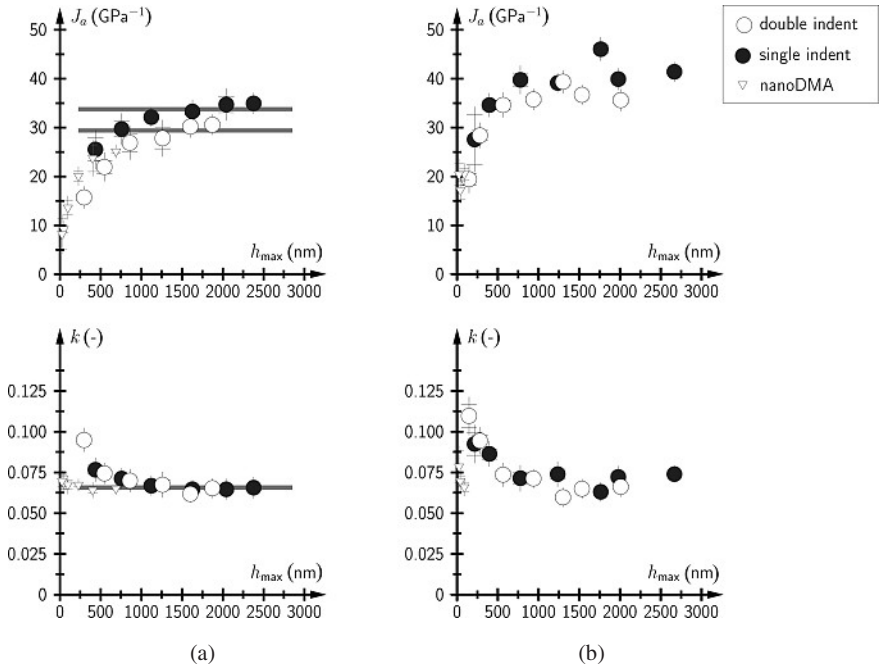

Fig. 8. Fractional dash-pot parameters for LDPE obtained from cyclic nanoindentation testing compared with parameters determined via single- and double-indentation testing using (a) a Berkovich tip and (b) a cono-spherical tip for different values h_{max}.

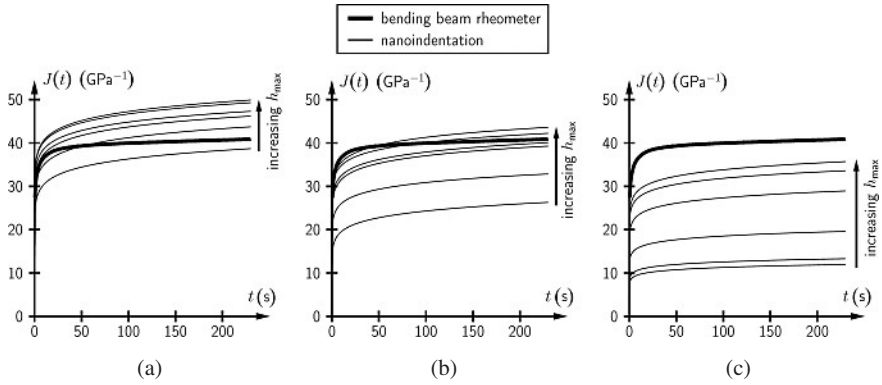

Fig. 9. Creep-compliance function for LDPE using model parameters identified by nanoindentation testing using the Berkovich tip and different maximum loads compared with the creep-compliance function obtained from bending-beam-rheometer tests: (a) Single-indentation technique, (b) double-indentation technique, and (c) cyclic testing.

(see Table 1) is plotted using the parameters obtained from different techniques and penetration depths (see Fig. 9) and compared with the creep-compliance function obtained from bending-beam-rheometer tests [23]. The creep-compliance function corresponding to the model parameters identified via the single-indentation technique slightly overestimates the macroscopic test results. This effect is explained by the plastic deformations occurring during the loading phase, which are not taken into account during parameter identification. The results obtained from double indentation, on the other hand, agree well with the bending-beam-rheometer test results, approaching the macroscopic creep compliance with increasing penetration. The creep-compliance functions identified via cyclic testing, corresponding to the different load levels, show the same increase in compliance with increasing penetration, highlighting the influence of the LDPE microstructure on the mechanical behavior.

5. Summary and conclusions

The identification of viscoelastic model parameters from cyclic nanoindentation tests was dealt with in this paper. Results from cyclic testing of low-density polyethylene (LDPE) using a Berkovich and a cono-spherical tip were presented. The parameters for the fractional dash-pot, describing the viscoelastic behavior of LDPE, were identified from back-calculation using the measured complex shear modulus. The obtained results are compared with parameters obtained from nanoindentation (static) creep tests using the single- and double-indentation technique. Furthermore, the creep-compliance function $J(t)$ of the fractional dash-pot corresponding to the parameters obtained from the different techniques was assessed by the creep-compliance function obtained from bending-beam-rheometer tests [23]. Based on the so-obtained results, the following conclusions can be drawn:

1. The fractional dash-pot is well suited for the description of the viscoelastic behavior of LDPE over the frequency range considered in the experimental program.
2. The model parameters obtained from cyclic testing agree well with the parameters identified by nanoindentation (static) creep tests using the double-indentation technique. The model parameter representing the initial creep compliance obtained from single-indentation tests, on the other hand, slightly overestimates the creep compliance obtained from the other two methods. This was explained by the effect of plastic deformation, which is not taken into account during parameter identification within the single-indentation technique.

3. The creep-compliance function computed using the obtained model parameters increased for all three methods with increasing penetration, showing the influence of the LDPE microstructure and, thus, the length scale of testing, on the identified model parameters. The parameters determined via single indentation lead to a creep-compliance function overestimating the creep-compliance function obtained from bending-beam-rheometer tests. The creep-compliance function corresponding to the parameters identified via double indentation and cyclic testing, on the other hand, showed good agreement with the macroscopic properties, approaching the macroscopic creep-compliance function with increasing penetration. This result underlines the good performance of the latter two methods.

In summary, cyclic testing was found to be appropriate for the identification of viscoelastic model parameters and the obtained results are in good agreement with the parameters obtained from nanoindentation (static) creep tests.

The authors thank all other members of the Christian Doppler Laboratory for "Performance-Based Optimization of Flexible Pavements" at Vienna University of Technology for helpful comments and fruitful discussions on the presented research work. Financial support by the Christian Doppler Gesellschaft (Vienna, Austria) is gratefully acknowledged.

References

[1] W.C. Oliver, G.M. Pharr: J. Mater. Res. 7 (1992) 1564.
[2] L. Cheng, X. Xia, W. Yu, L.E. Scriven, W.W. Gerberich: J. Polymer Sci., Part B: Polymer Physics 38 (2000) 10.
[3] L. Cheng, X. Xia, L.E. Scriven, W.W. Gerberich: Mech. Mater. 37 (2005) 213.
[4] P.-L. Larrson, S. Carlsson: Polymer Testing 17 (1998) 49.
[5] M. Sakai, S. Shimizu: J. Non-Cryst. Solids 282 (2001) 236.
[6] H. Lu, B. Wang, J. Ma, G. Huang, H. Viswanathan: Mech. Time-Dep. Mater. 7 (2003) 189.
[7] Y.-T. Cheng, C.-M. Cheng: Mater. Sci. Eng. R 44 (2004) 91.
[8] A. Jäger, R. Lackner, J. Eberhardsteiner: Mecanica 42 (2007) 293.
[9] E.H. Lee, J.R.M. Radok: J. Appl. Mech. 27 (1960) 438.
[10] J.B. Pethica, W.C. Oliver: Physica Scripta T 19 (1987) 61.
[11] J.L. Loubet, B.N. Lucas, W.C. Oliver: in: International Workshop on Instrumented Indentation, D. Smith (Ed.), San Diego, CA (1995) 31.
[12] S.A. Syed Asif, K.J. Wahl, R.J. Colton: Rev. Sci. Instrum. 70 (1999) 2408.
[13] S.A. Syed Asif, K.J. Wahl, R.J. Colton, O.L. Warren: J. Appl. Phys. 90 (2001) 1192.
[14] S.A. Hayes, A.A. Goruppa, F.R. Jones: J. Mater. Res. 19 (2004) 3298.
[15] G.M. Odegard, T.S. Gates, H.M. Herring: Exp. Mechanics 45 (2005) 130.
[16] K. Park, S. Mishra, G. Lewis, J. Losby, Z. Fan, J.B. Park: Biomaterials 25 (2004) 2427.
[17] C.C. White, M.R. Vanlandingham, P.L. Drzal, N.-K. Chang, S.-H. Chang: J. Polymer Sci., Part B: Polymer Physics 43 (2005) 1812.
[18] X. Li, B. Bhushan: Mater. Charact. 48 (2002) 11.
[19] Hysitron Inc.: Triboindenter User Manual, Minneapolis, MN (2006).
[20] W.N. Findley, J.S. Lai, K. Onaran: Creep and Relaxation of Nonlinear Viscoelastic Materials, Dover Publications, New York (1989).
[21] http://www.matweb.com.
[22] N.P. Cheremisinoff: Handbook of Polymer Science and Technology: Performance Properties of Plastics and Elastomers, Vol. 2, Marcel Dekker, New York (1989).
[23] A. Jäger, R. Lackner: Strain (2007), accepted for publication.
[24] A. Jäger, R. Lackner, K. Stangl: Int. J. Mater. Res. 98 (2007) 404.

(Received October 24, 2007; accepted January 25, 2008)

Bibliography

DOI 10.3139/146.101706
Int. J. Mat. Res. (formerly Z. Metallkd.)
99 (2008) 8; page ■ – ■

ISSN 1862-5282

Correspondence address

Andreas Jäger
Institute for Mechanics of Materials and Structures
Vienna University of Technology
Karlsplatz 13/202, A-1040 Vienna, Austria
Tel.: +43 1 58 801 20 218
Fax: +43 1 58 801 20 299
E-mail: Andreas.Jaeger@tuwien.ac.at